

Received:

16 July 2017

Revised:

10 October 2017

Accepted:

7 December 2017

Cite as: Livy Laysandra, Meri Winda Masnona Kartika Sari, Felycia Edi Soetaredjo, Kuncoro Foe, Jindrayani Nyoo Putro, Alfin Kurniawan, Yi-Hsu Ju, Suryadi Ismadji. Adsorption and photocatalytic performance of bentonite-titanium dioxide composites for methylene blue and rhodamine B decoloration. *Heliyon* 3 (2017) e00488. doi: [10.1016/j.heliyon.2017.e00488](https://doi.org/10.1016/j.heliyon.2017.e00488)



CrossMark

Adsorption and photocatalytic performance of bentonite-titanium dioxide composites for methylene blue and rhodamine B decoloration

Livy Laysandra^a, Meri Winda Masnona Kartika Sari^a, Felycia Edi Soetaredjo^{a,*}, Kuncoro Foe^b, Jindrayani Nyoo Putro^c, Alfin Kurniawan^c, Yi-Hsu Ju^c, Suryadi Ismadji^{a,*}

^a Department of Chemical Engineering, Widya Mandala Surabaya Catholic University, Kalijudan 37, Surabaya 60114, Indonesia

^b Faculty of Pharmacy, Widya Mandala Surabaya Catholic University, Pakuwon City, Kalisari 1, Surabaya 60112, Indonesia

^c Department of Chemical Engineering, National Taiwan University of Science and Technology, No. 43, Sec 4, Keelung Rd, Da'an District, Taipei City 106, Taiwan

*Corresponding author.

E-mail addresses: felyciae@yahoo.com (F.E. Soetaredjo), suryadiismadji@yahoo.com (S. Ismadji).

Abstract

Bentonite – TiO₂ composites were prepared by impregnation of TiO₂ and bentonite, followed by microwave irradiation processes. The composites were characterized using FTIR, SEM, XRD, and nitrogen sorption methods. Anatase phase of TiO₂ in all composites are observed through XRD diffraction peaks and surface morphology of the composites. The adsorption and photocatalytic capabilities of the composites were tested in liquid phase adsorption of methylene blue and Rhodamine B. The adsorption and photocatalytic degradation experiments were conducted in the presence or absence of UV light irradiation. Langmuir and Freundlich models were employed to correlate the experimental adsorption data, and it was found that Langmuir gave better performance in correlating the experimental data. Modification of Langmuir equation to accommodate

photocatalytic degradation process was conducted, and the model could represent the experimental results very well.

Keywords: Environmental science, Materials science, Chemical engineering

1. Introduction

Dyes usually used by various kinds of industries to color their products. Several industries that intensively use dyes to color their products are textiles, foods, pharmaceuticals, cosmetics, paints, pigments, ceramics, etc. During the industrial processing, some of the excess dyes will end up as waste and will be discharged as industrial effluent [1]. Industrial effluents containing dyes are dangerous to the aquatic environment as well as to human being. Therefore, a proper treatment should be conducted before these kinds of effluents can be discharged to the water environment. The principal purposes of the treatment are to remove inorganic or organic contaminants, and other pathogens microorganisms from water, so human for their daily activities can safely use the water.

Different kinds of dyes, mostly are synthetic ones, are commercially available in the markets. Synthetic dyes are classified into several categories: basic or cationic dyes, the direct dyes, the acid dyes, premetallized dyes, sulfur dyes, azoic dyes, vat dyes, collective dyes, and dyes for fabricated fibers. Basic dyes are water-soluble cationic dyes applied to substrate with anionic character where electrostatic attractions are formed. Some examples of basic dyes are Methylene Blue, Rhodamine B Crystal Violet, Congo Red, Methyl Orange, etc. [2]. Some of these synthetic dyes have been known to have potential hazards to human health, and their effect is mainly carcinogenic, mutagenic and teratogenic [3].

Methylene blue is known as methylthioninium chloride is a basic cationic dye with the molecular formula $C_{16}H_{18}N_3SCl$. At room temperature, methylene blue is solid, odorless, dark green powder and gives blue solution if dissolved in water. This dye is usually used in biological and chemical processes [4]. Rhodamine B is a basic cationic dye with the molecular formula $C_{28}H_{31}ClN_2O_3$ has a moderate wash and light fastness properties of wool. It is also useful as an analytical reagent for the detection and determination of metals [5, 6, 7].

Methylene blue can cause some health problems such as eye burns, which may be responsible for permanent injury to the eyes of human and animals. On an inhalation, it can give short periods of rapid or difficult breathing, while ingestion through the mouth gives a burning sensation and may cause nausea, vomiting, profuse sweating, mental confusion, and methemoglobinemia [8]. The long-term exposure of Rhodamine B to human may cause in transient mucous membrane and skin irritation. Rhodamine B potentially induces mutagenic activity and pose an

adverse effect on aquatic life via obstructing light penetration and oxygen transfer [9].

Many dyes and other organic contaminants are tough to degrade in nature and require more advanced techniques for their removal [1]. The decolorization of dye has received much attention. Thus various chemical, physical and biological treatment methods have been developed for the removal of dyes from aqueous solutions. These treatments include precipitation, coagulation-flocculation, reverse osmosis, oxidation with ozone, chlorine or hydrogen peroxide, use of anion exchange membranes and bacterial cells [10]. Adsorption is one of the most promising and widely used techniques for the removal synthetic dyes from wastewater [3]. Adsorption has proven to be a promising and cost-effective method. The price of adsorbent is an important parameter that significantly influences the total cost of an adsorption process system. Therefore the search of alternative adsorbents with high adsorption capacities was still the focus of current studies [11].

Many kinds of non-conventional adsorbent materials have been tested for their adsorption ability to remove dyes. As alternative adsorbents, non-conventional materials must possess similar adsorption capability to those commercial adsorbents, eco-friendly production, and also abundantly available [12]. The most promising and the materials as the candidate for alternative adsorbents are clay minerals. Bentonite is a clay material that can be found in many places around the world, including in Indonesian. Bentonite is a smectite mineral composed of aluminum silicate framework, and it has a layer structure with negative charge evenly across its surface and possesses good cation exchange.

In the last few years, the study of decolorization of dyes using photocatalytic process has been investigated [13]. Among different kinds of photocatalysts, TiO₂ is the most widely used for wastewater treatment because of its high oxidizing properties, super hydrophilicity and chemical stability [14]. However, this process requires UV-light radiation to promote the electron from the valence band to the conduction band and leave the hole (h⁺) in the valence band. If the hole meets the water molecule in the presence of oxygen, it will produce hydroxyl radical (OH[•]), and this hydroxyl radical will break down the organic molecule into the simple compound [13]. The main drawback of using titanium as a photocatalyst is its susceptibility to aggregation, reducing the surface area and efficiency [1]. To avoid this problem, a suitable material as the support to immobilize titanium particles should be developed, and clay materials are good candidates for this purpose [1].

In this study, bentonite was employed as the support to immobilize TiO₂ particles. The bentonite – TiO₂ composite was subsequently used to adsorb and degrade Methylene Blue and Rhodamine B. The adsorption, and photodegradation performances of the adsorbents were observed at various temperatures. Since the removal of Methylene Blue and Rhodamine B involves both of adsorption and

photodegradation, a modification of Langmuir equation was also conducted to represent the photo-degradation term.

2. Materials and methods

2.1. Materials

Ca-Bentonite used in this study was obtained from Pacitan, East Java, Indonesia. Titanium dioxide (anatase phase) was purchased from Degussa. Methylene Blue (MB) and Rhodamine B (RhB) were purchased from Merck, Germany.

2.2. Preparations of bentonite-titanium dioxide composite

Before use as the adsorbent, the bentonite was purified using H_2O_2 solution. The purification of bentonite was conducted to remove organic impurities. The purification was carried out in a sonicator for 6 hours at room temperature. After the purification process had completed, bentonite was separated from the solution and repeatedly washed with reverse osmosis water and dried in a forced circulation oven (Memmert) at 105 °C for 24 h. The purified bentonite was pulverized in a hammer mill and sieved using vibration screener (Retsch AS-200) to obtain a particle size of 100/120 mesh.

Bentonite titanium dioxide nanocomposites (BTC) were synthesized at a different weight ratio of TiO_2 (5, 10, 20%) using impregnation method [15]. The impregnation procedure is as follows: a known amount of titanium dioxide was dispersed in water; subsequently, a known amount of bentonite was added to the mixture and heated at 100 °C for 1 hour under continuous stirring. The BTC mixture was then irradiated using a microwave oven at 700W for 10 minutes. After the irradiation process had completed, the BTC was separated from the liquid and dried at 105 °C for 24 h. The radiation process using microwave could improve the adsorption capacity of adsorbent [16].

2.3. Characterizations of materials

The characterizations of bentonite and nanocomposites were conducted using several methods such surface charge, FTIR (Fourier Transform Infra-Red Spectrophotometry), SEM (Scanning Electron Microscopy), and XRD (X-Ray Diffraction). In this study, the surface charge of bentonite and nanocomposites was measured by a zeta meter (Zeta Potential Analyzer, Brookhaven 90Plus). The pH_{pzc} (the pH where the adsorbent has no charge) or isoelectric points of bentonite and nanocomposites were 3.9 (bentonite (B)), 5.2 (B + 5% TiO_2), 6.1 (B + 10% TiO_2), and 7.6 (B + 20% TiO_2).

The FTIR analysis of bentonite and nanocomposites were conducted on a Shimadzu FTIR 8400S spectrometer using KBr method. The FTIR spectra of the

samples were acquired at a wavenumber of 4000 to 500 cm^{-1} . The FTIR data were collected in transmission mode. The adjustment of the baseline, normalization, and smoothing of the FTIR spectra were conducted using IRsolution software package (version 1.21). This software is available in the FTIR instrument.

The surface morphologies of bentonite and titanium nanocomposites were determined by scanning electron microscopy method. The surface analysis was carried out on a JEOL JSM-6500F field emission SEM at 20 kV. Before SEM analysis, the samples were coated with a thin layer of platinum (3 nm). The coating process was conducted for 90 s in argon atmosphere using a fine auto coater (JFC-1600, JEOL, Ltd., Japan).

X-ray diffraction patterns of the samples were obtained at 40 kV and 30 mA using XRD, Philips X'pert X-ray Diffractometer. Monochromatic high-intensity Cu $K\alpha 1$ ($\lambda = 0.15405$ nm) was employed as the source of radiation. The pore structures of the samples were characterized by nitrogen sorption analysis. The nitrogen sorption measurements were conducted at the boiling point of nitrogen gas (-176 °C) using Micromeritics ASAP 2010 sorption analyzer. The adsorption and desorption of the nitrogen were performed at relative pressure (p/p°) range of 0.005 to 0.995. The degassing of the samples were conducted at 200 °C under high vacuum condition.

2.4. Adsorption and photocatalytic degradation experiment

Adsorption and photocatalytic processes were carried out isothermally in a water bath shaker that has been modified by adding a UV lamp as the light source. The adsorption and photodegradation processes were conducted with an initial concentration of 200 ppm for both MB and RhB. For the isotherm process, the various mass of Ca-bentonite or BTC (0.1 – 0.9 g) were added to a series of iodine flasks, each flask containing 100 mL of MB or RhB solution. The adsorption and photodegradation experiments were performed at three different temperatures (30 °C, 50 °C, and 70 °C) and pH 8. During the experiments, the iodine flasks containing the mixture were shaken in a thermal controlled shaking water bath (Memmert WB-14) with constant speed at 100 rpm for 2 h at desired temperature with/without UV irradiation at 360 nm (To measure the adsorption performance of the composites, the adsorption experiments was conducted in the dark without any light disturbing.). After the adsorption and photodegradation process had completed, samples were centrifuged (Heraeus Labofuge 200) at 3500 rpm for 2 min to separate the solution from the adsorbent [11]. The initial and equilibrium concentrations of MB or RhB were determined by UV-Visible spectrophotometer (UV mini 1240 Shimadzu) at the maximum wavelength (664.1 nm for MB and 554.0 nm for RhB).

The amount of MB or RhB adsorbed by the adsorbent at equilibrium condition was determined by equation (1) as follow:

$$q_e = \frac{(C_0 - C_e)}{m} \times V \quad (1)$$

Where q_e is the amount of MB or RhB adsorbed at equilibrium (mmol/g), C_0 and C_e (mmol/L) represent the concentration of MB or RhB in the liquid phase at initial and equilibrium condition, respectively. The volume of MB or RhB solution is represented by symbol V (L) and m is the mass of adsorbent (g).

3. Results and discussion

3.1. FTIR analysis

In this study, FTIR spectroscopy was used to analyze the functional groups of the adsorbents. Fig. 1. Shows the FTIR spectra of TiO_2 , bentonite, B + 5% TiO_2 , B + 10% TiO_2 , and B + 20% TiO_2 . Broadband around 500 to 700 cm^{-1} possibly due to the vibration of Ti-O bonds in the titanium dioxide lattice [17]. The vibration of hydroxyl groups is observed at broad peaks around 3100 to 3600 cm^{-1} (Fig. 1a). Typical infrared absorption bands of montmorillonite are observed on the bentonite (Fig. 1e). Those bands are Al(Mg) – O – H stretching (3620 cm^{-1}), intermolecular hydrogen-bonded H – O – H stretching (3343 cm^{-1}), Si–O–Si stretching vibration at 1113 cm^{-1} , Al-OH (911 cm^{-1}), (Al, Mg)–O (866 cm^{-1}), and Si–O bending vibration (445 cm^{-1}) [18]. Similar infrared absorption bands of montmorillonite and TiO_2 are observed for all of the bentonite – TiO_2 composites as seen in Fig. 1. Skeletal vibrations of clay particles and TiO_2 for all composites are in the wavenumbers between 1200–450 cm^{-1} [17].

3.2. Surface morphology analysis

The surface morphology of bentonite and composites (B + 5% TiO_2 , B + 10% TiO_2 , and B + 20% TiO_2) was examined by SEM, and the results are depicted in Fig. 2. From this Figure, it can be seen that bentonite possesses different surface morphology with bentonite – TiO_2 composites. The surface morphology of bentonite appears as a flake-like structure with a smooth surface in some part of the particles, while the bentonite – TiO_2 composite, some TiO_2 particles have been incorporated into the surface of bentonite (smaller TiO_2 grains on the outer face of bentonite). The EDS spectra reveal that the composite contains a significant amount of titanium as indicated in Fig. 2.

3.3. X-ray diffraction

Fig. 3 shows the XRD patterns of bentonite and bentonite – TiO_2 nanocomposites. Based on the XRD pattern of bentonite, the specific diffraction peak for

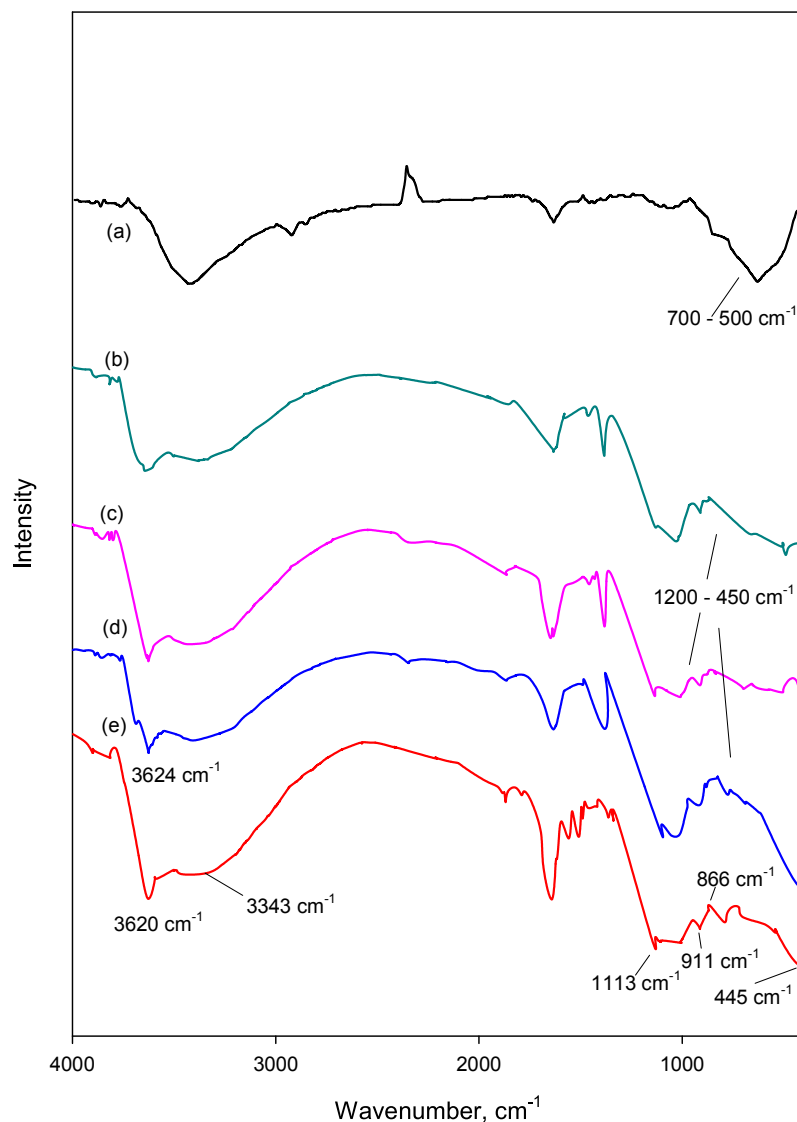


Fig. 1. FTIR spectra of (a) TiO₂, (b) B + 20% TiO₂, (c) B + 10% TiO₂, (d) B + 5% TiO₂, and (e) Ca-bentonite.

montmorillonite appears at $2\theta = 5.69^\circ$, and this 2θ corresponds to the basal spacing $d_{001} = 15.53 \text{ \AA}$. Other characteristic diffraction peaks of montmorillonite were observed at $2\theta = 19.82^\circ$, 27.70° , 34.79° , and 59.64° . The presence of quartz on the bentonite was also observed, and the diffraction peaks of quartz were found at $2\theta = 26.59^\circ$ and 50.01° .

The specific diffraction peak of montmorillonite in composites was observed at 2θ around 5.40° (B + 5%TiO₂), 5.29° (B + 10%TiO₂), and 5.19° (B + 20%TiO₂). Incorporation of TiO₂ into bentonite structure slightly increases the interlayer spacing from 15.53 \AA to 16.35 \AA (B + 5%TiO₂), 16.71 \AA (B + 10%TiO₂), and 17 \AA . The increase of interlayer spacing with the increase of TiO₂ ratio possibly due to

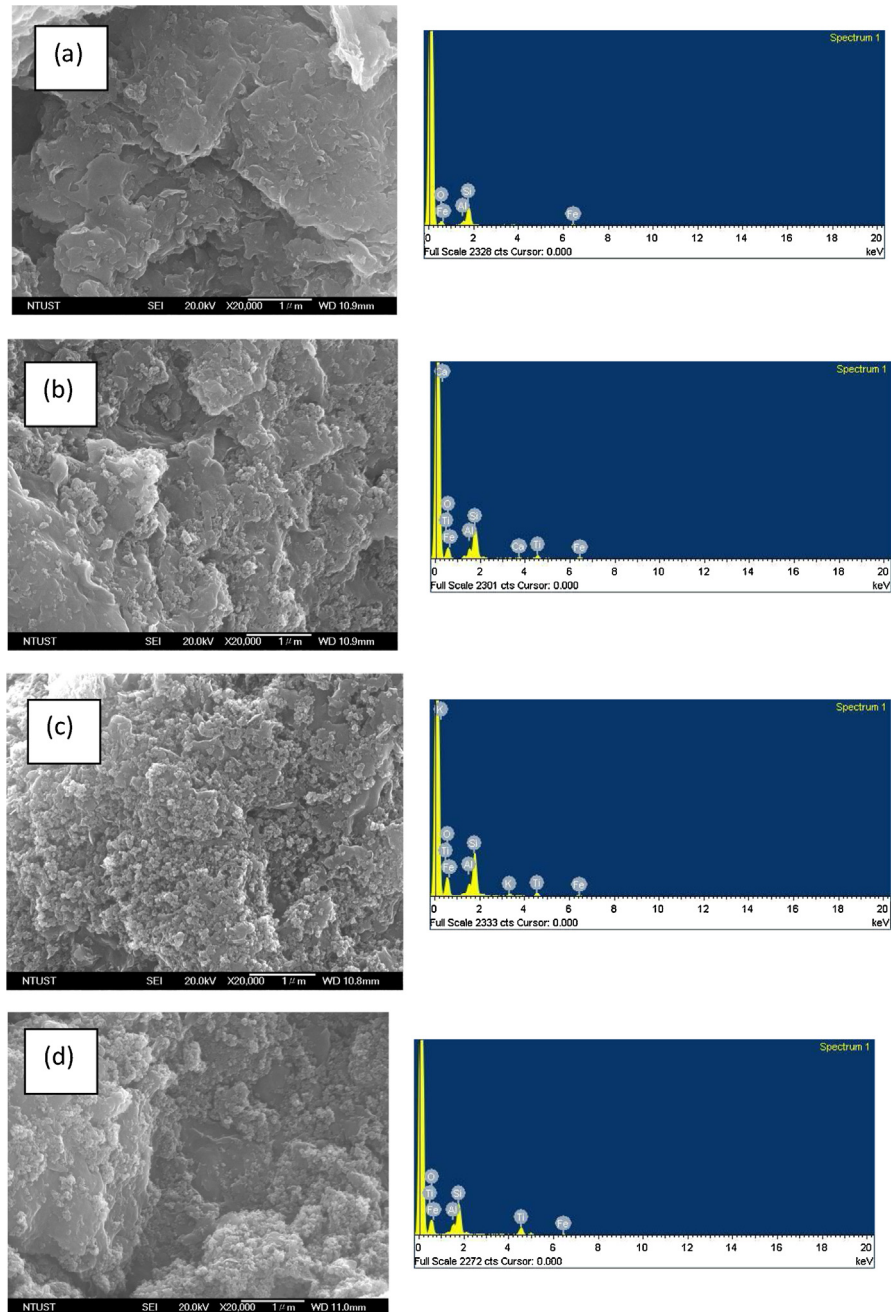


Fig. 2. SEM images and EDS spectra of (a) bentonite, (b) B + 5% TiO₂, (c) B + 10% TiO₂, and (d) B + 20% TiO₂.

the exchanged of Na⁺ or Ca²⁺ with TiO₂. More TiO₂ particles were available with the increase of TiO₂ ratio, and more particles penetrated into the bentonite interlayers (due to the ion-exchanged process) increasing interlayer spacing. Anatase phase of TiO₂ in all composites are observed through diffraction peaks around $2\theta = 25.50^\circ$ (101), 37.69° (112), 48.15° (200), and 54.99° . This evidence

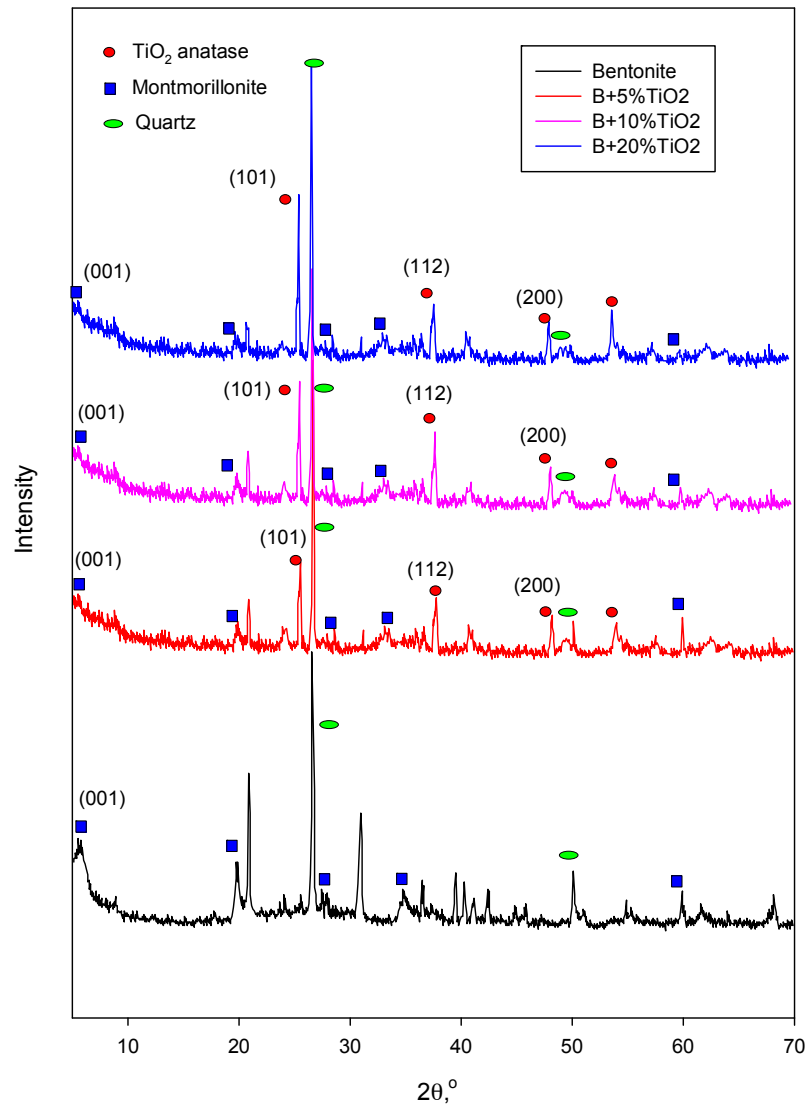


Fig. 3. X-ray diffraction of bentonite and composites.

indicates that there is no change in the phase of TiO_2 during the microwave irradiation process. Anatase phase of TiO_2 has much higher photocatalytic activity than other phases of TiO_2 .

3.4. Nitrogen sorption measurements

The nitrogen sorption isotherms for bentonite and bentonite – TiO_2 composites are given in Fig. 4. The adsorption isotherm of bentonite (Fig. 4a) indicates that this material possesses some amount of micropore in its structure. Rapid intake of nitrogen gas by the solid at very low relative pressure (p/p°) is the characteristic of the solid that has some microporous structure (type I adsorption isotherm). With the increase of relative pressure, the isotherm becomes type II, and wide hysteresis

loop is observed as seen in Fig. 4a. This kind of hysteresis loop can be considered as H2 type hysteresis. This hysteresis indicates that the purification of natural bentonite with concentrated hydrogen peroxide solution created some complex network of interconnected pores or interlayers with bottleneck and contractions [19], and such structure delayed the desorption of nitrogen gas. The BET surface area and pore volume of the bentonite are $68.4 \text{ m}^2/\text{g}$ and $0.126 \text{ cm}^3/\text{g}$, respectively.

The nitrogen sorption isotherms of the composites are given in Fig. 4b, c, and d. The sorption isotherms of composites B + 5% TiO_2 and B + 10% TiO_2 are similar to the bentonite, combination between type I and II. Type II isotherms indicate that B + 5% TiO_2 and B + 10% TiO_2 contain both mesoporous and macroporous structures. The BET surface area and pore volume of composite B + 5% TiO_2 are $111.7 \text{ m}^2/\text{g}$ and $0.191 \text{ cm}^3/\text{g}$, respectively, while for B + 10% TiO_2 are $141.8 \text{ m}^2/\text{g}$ and $0.218 \text{ cm}^3/\text{g}$. With the addition of TiO_2 , some ion exchange process between Na^+ and Ca^{2+} with TiO_2 occurred, and some interlayer which initially inaccessible by nitrogen gas now become available due to the penetration of titanium molecules, so it enhances the

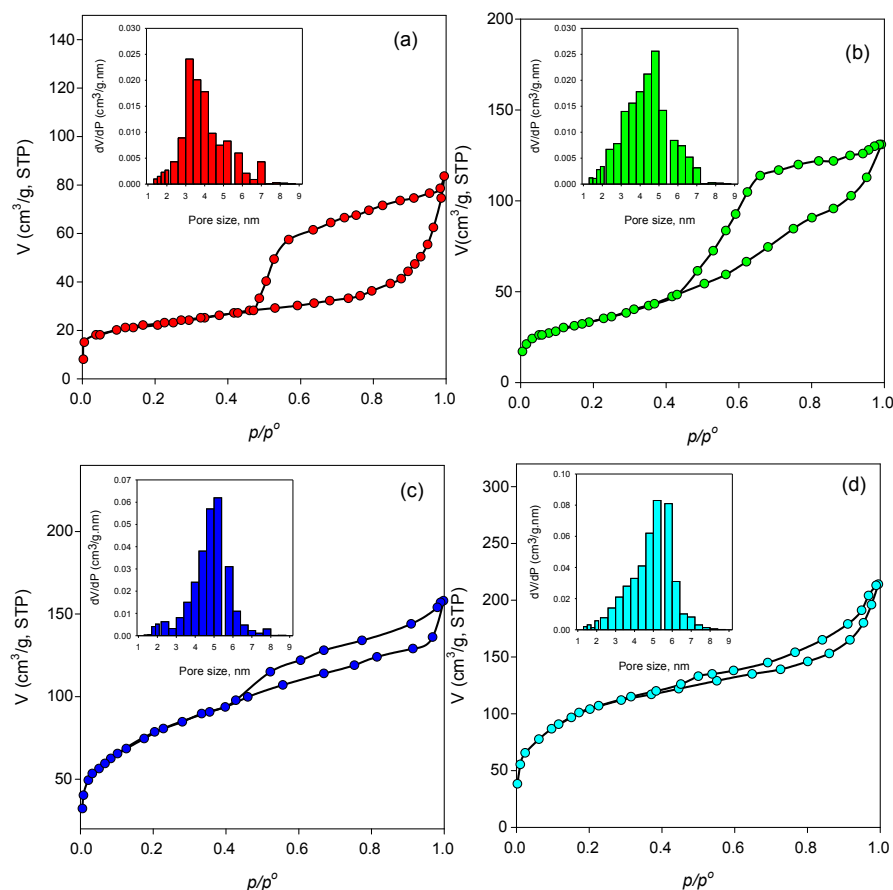


Fig. 4. Nitrogen sorption isotherms and pore size distribution for (a) bentonite, (b) B + 5% TiO_2 , (c) B + 10% TiO_2 , and (d) B + 20% TiO_2 .

adsorption of nitrogen. With the increase of the ratio of TiO₂ to 20%, the type of sorption isotherms of the composites change from type I/II to type IV with H3-H4 hysteresis loop as depicted in Fig. 4d. It indicates that B + 20% TiO₂ contain non-rigid aggregates of plate-like particles with a contribution of micropores and mesopores [20]. The BET surface area of B + 20% TiO₂ composite is 208.6 m²/g and total pore volume 0.243 cm³/g. The pore size distribution (PSD) of bentonite and composites were obtained by density functional theory (DFT) with medium regularization; the results are also given in Fig. 4 (as insert graphics). The PSDs reveal that all of the solids mainly have mesoporous structures.

3.5. Adsorption and photocatalytic performance

Analysis of the adsorption isotherm is very crucial for the design of adsorption system. The adsorption isotherm describes how the adsorbate molecules interact with the adsorbent surface at equilibrium condition [21]. Currently, many adsorption isotherm equations are available to represent the experimental adsorption data of different systems, and the most widely used equations to represent the liquid phase adsorption experimental data are Langmuir and Freundlich equations. In this study, we also employed Langmuir and Freundlich isotherms to represent the adsorption data of MB and RhB onto bentonite and composites (the adsorption experiments were carried out in the dark place without UV irradiation). The mathematical expressions of Langmuir and Freundlich adsorption models are given in Eqs. (2) and (3):

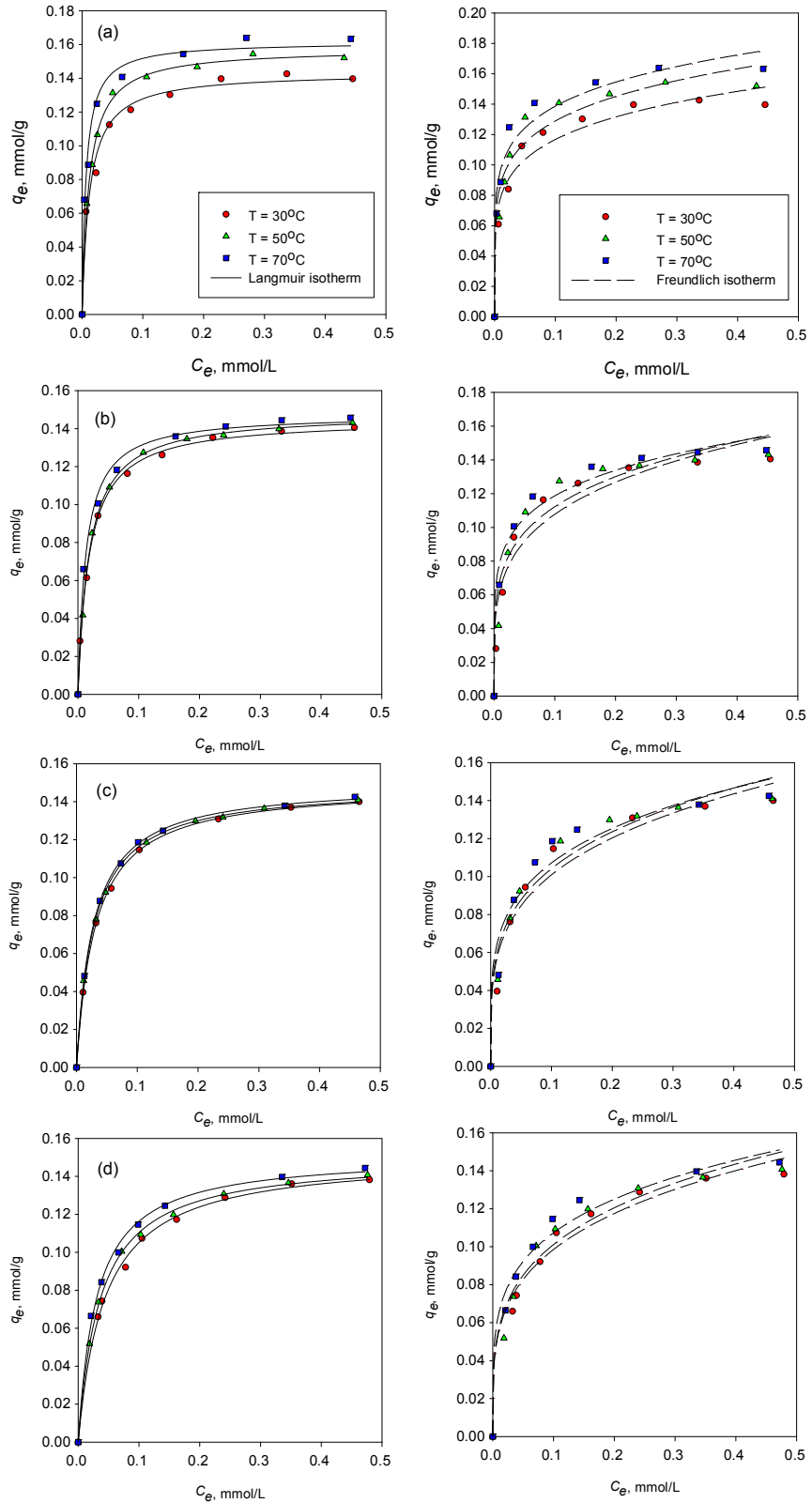
$$q_e = q_{\max} \frac{K_L C_e}{1 + K_L C_e} \quad (2)$$

Where q_e and C_e are the amount of dyes adsorbed by the adsorbent at equilibrium condition and equilibrium concentration, respectively. The Langmuir parameters q_{\max} and K_L represent the maximum adsorption capacity and adsorption affinity.

$$q_e = K_F C_e^{1/n} \quad (3)$$

Where K_F and n are Freundlich constants that represent the adsorption capacity of the adsorbent and heterogeneity of the system, respectively.

The adsorption isotherms of MB and RhB onto bentonite and composites are given in Figs. 5 and 6. In this figure, the experimental adsorption data are represented by the symbols, while the theoretical isotherms are given by solid (Eq. (2)) and dash (Eq. (3)) lines. The parameters of Langmuir and Freundlich equation obtained from the fitting of the experimental data with the isotherm models are summarized in Table 1 (MB) and Table 2 (RhB). From Figs. 5 and 6, it is evident that the Langmuir equation can represent the experimental data better than Freundlich equation. Langmuir equation also has better values of R^2 compared to Freundlich equation (Tables 1 and 2).



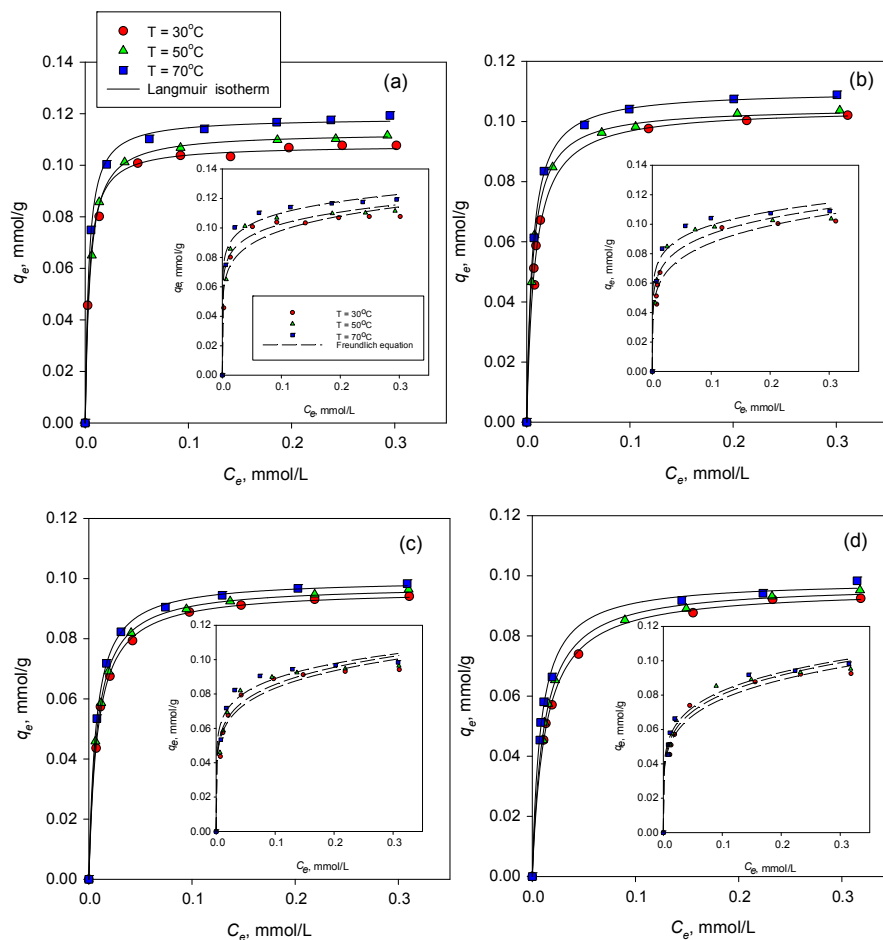


Fig. 6. Experimental and theoretical adsorption isotherms of RhB onto (a) bentonite, (b) B + 5% TiO₂, (c) B + 10% TiO₂, and (d) B + 20% TiO₂.

Comparing the adsorption capacity of the solids, without the presence of UV light the ratio of TiO₂ on composite did not give any contribution to the adsorption capacity as seen in Tables 1 and 2, the value of q_{\max} for all adsorbents are essentially constant. From Figs. 5 and 6, it can be seen that temperature gives a positive contribution to the amount of dyes adsorbed by the adsorbents. The amount uptake slightly increases with the increase of temperature. The increase of the adsorption capacity with temperature indicates that the chemisorption controls the adsorption of MB and RhB onto bentonite and composites.

Since the Langmuir could represent the experimental adsorption data better than Freundlich model, the Langmuir equation was modified to include the photocatalytic degradation term. With the presence of UV light during the adsorption process, the decrease of the amount of dyes during the process is due to the adsorption and

Fig. 5. Experimental and theoretical adsorption isotherms of MB onto (a) bentonite, (b) B + 5% TiO₂, (c) B + 10% TiO₂, and (d) B + 20% TiO₂.

Table 1. Langmuir and Freundlich parameters for the adsorption of MB onto bentonite and composites without UV irradiation.

Adsorbent	T(°C)	Langmuir Parameters			Freundlich Parameters		
		q_m (mmol/g)	K_L (L/mmol)	R^2	K_f (mmol/g (mmol/L) ⁻ⁿ)	n	R^2
Bentonite	30	0.1434	82.06	0.993	0.1741	5.76	0.984
	50	0.1576	86.09	0.998	0.1911	5.86	0.977
	70	0.1615	156.09	0.992	0.1992	6.36	0.969
B+ 5% TiO ₂	30	0.1450	59.94	0.997	0.1850	4.26	0.942
	50	0.1482	54.96	0.999	0.1834	4.69	0.939
	70	0.1476	77.12	0.994	0.1771	5.75	0.978
B+ 10% TiO ₂	30	0.1486	32.31	0.998	0.1813	3.93	0.958
	50	0.1484	35.34	0.995	0.1839	4.06	0.965
	70	0.1497	36.47	0.996	0.1805	4.41	0.951
B+ 20% TiO ₂	30	0.1508	23.02	0.997	0.1768	3.95	0.980
	50	0.1500	27.89	0.996	0.1810	3.95	0.968
	70	0.1515	33.14	0.997	0.1782	4.54	0.982

Table 2. Langmuir and Freundlich parameters for the adsorption of RhB onto bentonite and composites without UV irradiation.

Adsorbent	T (°C)	Langmuir Parameters			Freundlich Parameters		
		q_m (mmol/g)	K_L (L/mmol)	R^2	K_f (mmol/g (mmol/L) ⁻ⁿ)	n	R^2
Bentonite	30	0.1078	272.97	0.996	0.1350	7.25	0.962
	50	0.1127	231.65	0.996	0.1325	9.03	0.975
	70	0.1184	297.29	0.998	0.1384	10.08	0.987
B+ 5% TiO ₂	30	0.1044	127.41	0.993	0.1329	5.49	0.937
	50	0.1047	174.46	0.998	0.1335	6.45	0.962
	70	0.1102	180.14	0.999	0.1335	7.81	0.978
B+ 10% TiO ₂	30	0.0963	120.97	0.992	0.1218	6.07	0.968
	50	0.0978	130.29	0.993	0.1234	6.28	0.970
	70	0.0997	149.38	0.998	0.1214	7.41	0.975
B+ 20% TiO ₂	30	0.0957	80.81	0.999	0.1211	5.19	0.983
	50	0.0971	91.11	0.998	0.1239	5.31	0.980
	70	0.0983	123.05	0.997	0.1241	5.62	0.987

photocatalytic degradation processes. Before the photocatalytic degradation process occurs, the first process is the adsorption of dye molecules on the surface of the composite. When the dye molecules adsorbed on the surface near the TiO₂ particles, with the presence of UV light, the photocatalytic degradation process occurs. The degradation process is initiated by the excitation of an electron from the valence band of the TiO₂ catalyst to the conduction band, thus generating a hole (h^+) in the valence band and make $\bullet\text{OH}$ radical when contacted with water. Subsequently, the $\bullet\text{OH}$ radical attacks dye molecule and degradation process occur. After the degradation of dye molecule has finished, some of the degradation product will be released to water, and some possibly remain adsorbed on the surface of the adsorbent. This process continues until the product of degradation covers the TiO₂ particle and become deactivated. However, if dye molecules are adsorbed on the surface far from the location of TiO₂ particle, the photocatalytic degradation process will not occur. The photocatalytic degradation process enhances the uptake of dye molecules by the adsorbent. Therefore the adsorption capacity of the adsorbent (q_{max}^*) will increase. Since the adsorption and photocatalytic degradation processes occur simultaneously, the adsorption affinity is a combination between chemical reaction process and chemical or physical adsorption. Therefore, energy of adsorption is a sum of isosteric heat of adsorption and heat of chemical reaction, now in the temperature dependent form the adsorption affinity can be written as

$$K_L = K_L^o \exp \left[\frac{-Q}{RT} + \frac{-\Delta H}{RT} \right] \quad (4)$$

In Eq. (4), K_L^o is a Langmuir constant at reference temperature that combines both of adsorption and photocatalytic degradation process, R and T are ideal gas constant and temperature of adsorption, respectively. Isosteric heat of adsorption is represented by symbol Q and heat of chemical reaction is given by symbol ΔH .

It is evident (Fig. 2) that not all the surface of bentonite in the composites are covered by TiO₂ particles in where the photocatalytic degradation process occurs, and some part of the surface still available for only the adsorption process. If the available space for adsorption and photocatalytic degradation process is called as the active site; the fraction of the active site for adsorption alone is θ_{ad} and for simultaneous adsorption and photocatalytic degradation is θ_{deg} (Eq. (5)),

$$\theta_{ad} + \theta_{deg} = 1 \quad (5)$$

Each of the available processes (adsorption or photocatalytic degradation) contributes a certain amount of energy on the adsorption affinity, the contribution is linear with the fraction of each active site, and Eq. (5) can be rewritten as Eq. (6):

$$K_L = K_L^o \exp \left[\frac{-Q}{RT} \theta_{ad} + \frac{-\Delta H}{RT} \theta_{deg} \right] \quad (6)$$

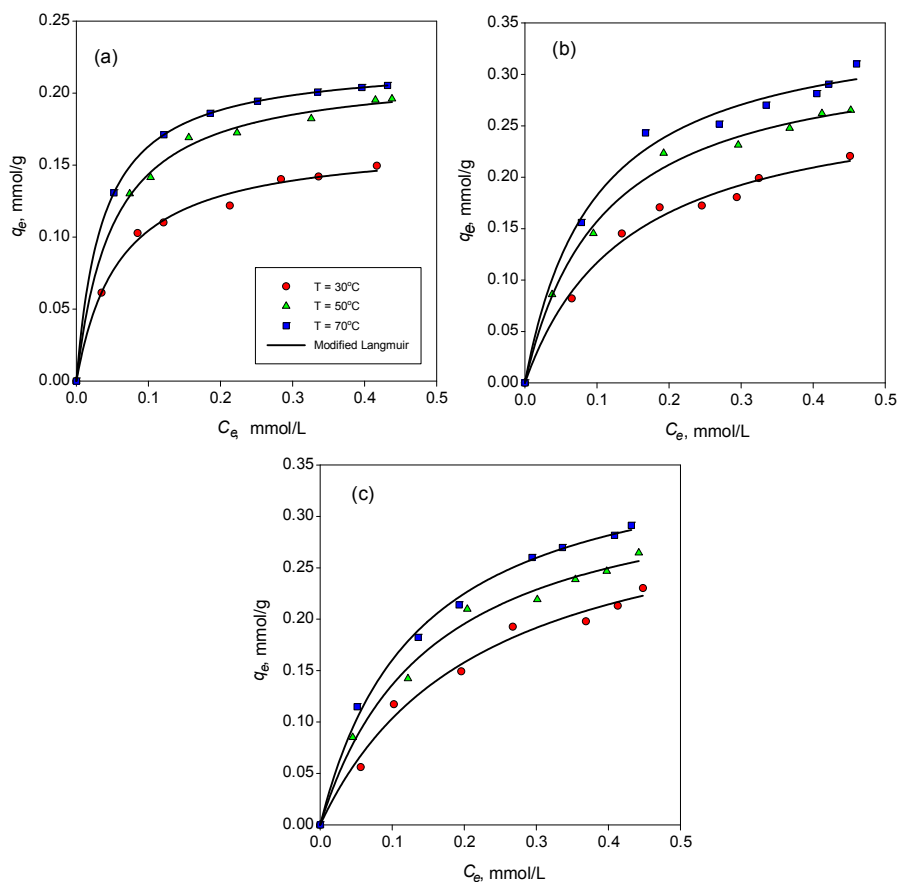


Fig. 7. Adsorption isotherms and theoretical modified Langmuir model on the adsorption of MB under UV light irradiation. (a) B + 5% TiO₂, (b) B + 10% TiO₂, and (c) B + 20% TiO₂.

Substitution of Eq. (5) into (6) produces Eq. (7)

$$K_L = K_L^o \exp \left[\frac{-Q}{RT} \theta_{ad} + \frac{-\Delta H}{RT} (1 - \theta_{ad}) \right] \tag{7}$$

The modified Langmuir equation for adsorption and photocatalytic degradation can be written as

$$q_e^* = q_{max}^* K_L^o \exp \left[\frac{-Q}{RT} \theta_{ad} + \frac{-\Delta H}{RT} (1 - \theta_{ad}) \right] C_e / \left(1 + K_L^o \exp \left[\frac{-Q}{RT} \theta_{ad} + \frac{-\Delta H}{RT} (1 - \theta_{ad}) \right] C_e \right) \tag{8}$$

Where q_e^* in Eq. (8) is the pseudo-total amount of dye adsorbed and degraded at equilibrium condition.

Figs. 7 and 8 show the experimental adsorption data of MB and RhB onto composites under UV light irradiation. Theoretical plots of Eq. (8) are also given in those figures. It is evident that the modified Langmuir equation can represent the experimental adsorption data very well. The adsorption of MB and RhB onto

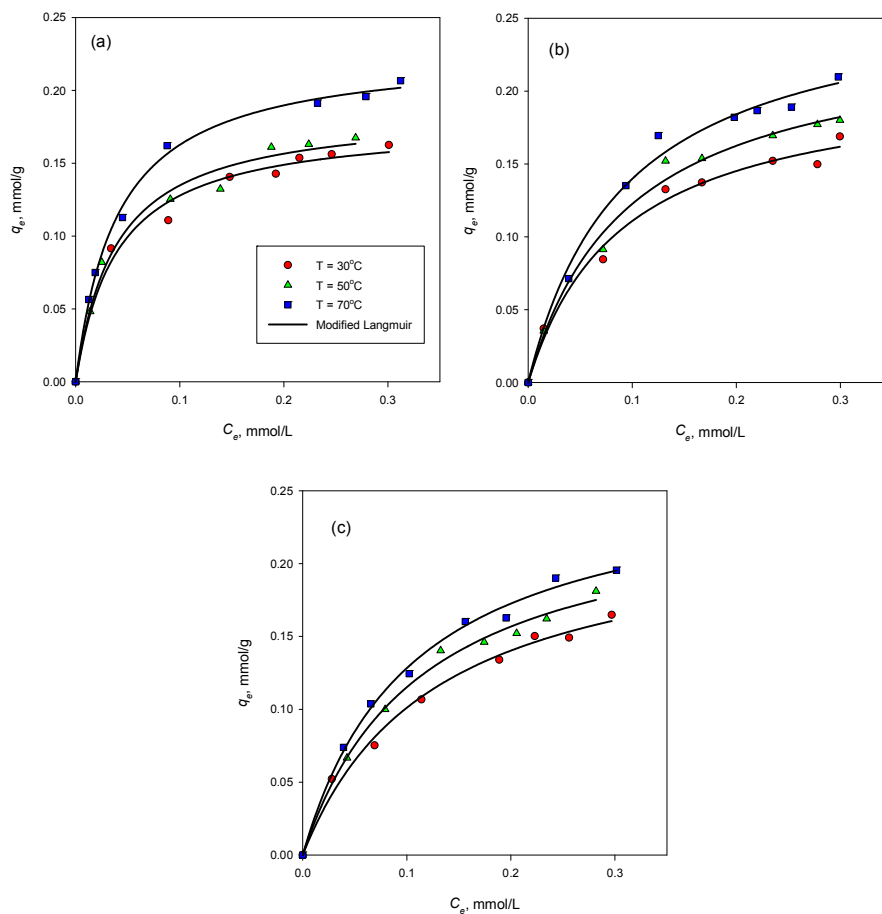


Fig. 8. Adsorption isotherms and theoretical modified Langmuir model on the adsorption of RhB under UV light irradiation. (a) B + 5% TiO₂, (b) B + 10% TiO₂, and (c) B + 20% TiO₂.

bentonite – TiO₂ composites under UV light irradiation can enhance the “adsorption capacity” of the composites more than 30%. The parameters of modified Langmuir equation obtained from the fitting of the experimental data are summarized in Tables 3 and 4. It is evident that the ratio of TiO₂ and temperature play a significant role in the removal of MB and RhB from aqueous solution.

The adsorption and photocatalytic degradation of MB and RhB onto composites are endothermic processes as indicated by positive values of Q and ΔH (Tables 3 and 4). Since both of adsorption and photocatalytic degradation are endothermic processes, the increase of temperature enhanced the amount uptake and degradation reaction. In general, the values of Q and ΔH are essentially independent of temperature but dependent on the adsorption system as seen in Tables 3 and 4. This phenomenon is consistent with many adsorption systems [22, 23].

The photocatalytic degradation of MB and RhB is a function of TiO₂ ratio. The fraction of the active site for photocatalytic degradation reaction (θ_{deg}) increased

Table 3. Modified Langmuir parameters for the adsorption of MB onto composites with UV irradiation.

Adsorbent	T (°C)	Parameters						
		q_m^* (mmol/g)	K_L° (L/mmol)	Q (kJ/mol)	ΔH (kJ/mol)	θ_{ad}	θ_{deg}	R^2
B+ 5% TiO ₂	30	0.2034	863.07	10.32	9.57	0.857	0.143	0.994
	50	0.2119	1050.80	9.97	10.17	0.771	0.229	0.997
	70	0.2228	1229.37	10.18	10.31	0.652	0.348	0.995
B+ 10% TiO ₂	30	0.2712	951.16	11.52	13.78	0.741	0.259	0.989
	50	0.3253	1215.62	11.91	13.56	0.569	0.431	0.995
	70	0.3506	1428.31	10.98	13.99	0.428	0.572	0.990
B+ 20% TiO ₂	30	0.3146	1098.75	12.34	14.96	0.539	0.461	0.986
	50	0.3423	1362.54	12.02	15.02	0.401	0.599	0.989
	70	0.3681	1567.85	11.98	14.75	0.298	0.702	0.991

Table 4. Modified Langmuir parameters for the adsorption of RhB onto composites under UV irradiation.

Adsorbent	T (°C)	Parameters						
		q_m^* (mmol/g)	K_L° (L/mmol)	Q (kJ/mol)	ΔH (kJ/mol)	θ_{ad}	θ_{deg}	R^2
B+ 5% TiO ₂	30	0.1798	988.25	8.54	12.81	0.813	0.187	0.995
	50	0.1938	1205.25	9.01	12.48	0.681	0.319	0.998
	70	0.2214	1398.14	8.77	12.16	0.593	0.407	0.992
B+ 10% TiO ₂	30	0.2074	1078.45	10.32	14.02	0.711	0.289	0.987
	50	0.2296	1251.44	9.88	13.75	0.531	0.469	0.991
	70	0.2414	1458.05	10.20	14.21	0.493	0.507	0.989
B+ 20% TiO ₂	30	0.2189	1152.39	11.06	14.95	0.652	0.348	0.991
	50	0.2374	1369.59	10.59	14.78	0.495	0.505	0.994
	70	0.2594	1523.23	10.84	14.56	0.386	0.614	0.995

with the increase of TiO₂ ratio. As mentioned before, the presence of TiO₂ in the solid system will initiate the formation of $\bullet\text{OH}$ radical and this radical acts as the active site for photocatalytic degradation reaction. With the increase in the number of TiO₂ particles (an increase of TiO₂ ratio), the number of free $\bullet\text{OH}$ radical also increase, and it enhanced the photocatalytic degradation of MB and RhB.

4. Conclusion

In this study, bentonite – TiO₂ composites were prepared by impregnation followed by microwave irradiation processes. Physical characteristics of the composites were determined using FTIR analysis, XRD, SEM, and nitrogen sorption methods. The

adsorption and photocatalytic degradation capability of the composites were tested against MB and RhB solution. The liquid phase adsorption experiment was conducted with or without UV light irradiation. The UV light irradiation process can enhance the uptake or degradation of MB and RhB more than 30% of the process without UV light irradiation. Langmuir and Freundlich adsorption equations were employed to correlate the experimental adsorption data, and Langmuir model gave a better representation than Freundlich. To accommodate the photocatalytic degradation process into the adsorption isotherm, the modification of Langmuir equation by the inclusion of heat of reaction and fraction of the active site for photocatalytic degradation process was conducted. The modified Langmuir model can represent the experimental data well with reasonable parameters values.

Declarations

Author contribution statement

Livy Laysandra and Meri Winda Masnona Kartika Sari: Performed the experiments.

Felycia Edi Soetaredjo: Conceived and designed the experiments; Wrote the paper.

Kuncoro Foe, Jindrayani Nyoo Putro and Alfin Kurniawan: Analyzed and interpreted the data.

Yi-Hsu Ju: Contributed reagents, materials, analysis tools or data; Wrote the paper.

Suryadi Ismadji: Conceived and designed the experiments; Contributed reagents, materials, analysis tools or data; Wrote the paper.

Funding statement

This work was supported by the Indonesia Ministry of Research and Technology and Higher Education through Competency Grant

Competing interest statement

The authors declare no conflict of interest.

Additional information

No additional information is available for this paper.

References

- [1] W. Hajjaji, S.O. Ganiyu, D.M. Tobaldi, S. Andrejkovičová, F.R.R.C. Pullar, J.A. Labrincha, Natural Portuguese clayey materials and derived TiO₂-

- containing composites used for decolouring methylene blue (MB) and orange II (OII) solutions, *Appl. Clay Sci.* 83–84 (2013) 91–98.
- [2] R. Djellabi, M.F. Ghorab, G. Cerrato, S. Morandi, S. Gatto, V. Oldani, A.D. Michele, C.L. Bianchi, Photoactive TiO₂–montmorillonite composite for degradation of organic dyes in water, *J. Photochem. Photobiol. A: Chem.* 295 (2014) 57–63.
- [3] H. Mittala, S.S. Raya, A study on the adsorption of methylene blue onto gum ghatti/TiO₂ nanoparticles-based hydrogel nanocomposite, *Int. J. Biol. Macromol.* 88 (2016) 66–80.
- [4] S. Li, Removal of crystal violet from aqueous solution by sorption into semi-interpenetrated networks hydrogels constituted of poly(acrylic acid-acrylamide-methacrylate) and amylose, *Biores. Technol.* 101 (2010) 2197–2202.
- [5] A.A. Attia, B.S. Girgis, N.A. Fathy, Removal of methylene blue by carbons derived from peach stones by H₃PO₄ activation: Batch and column studies, *Dyes Pigments* 76 (2008) 282–289.
- [6] P. Sharma, H. Kaur, M. Sharma, V. Sahore, A review on applicability of naturally available adsorbents for the removal of hazardous dyes from aqueous waste, *Environ. Monit. Assess.* 183 (2011) 151–195.
- [7] V.K. Gupta, I. Ali, V.K. Saini, Removal of Rhodamine B, Fast Green, and Methylene Blue from Wastewater Using Red Mud, an Aluminum Industry Waste, *Ind. Eng. Chem. Res.* 43 (2004) 1740–1747.
- [8] W.S.W. Ngah, M.A.K.M. Hanafia, Removal of heavy metal ions from wastewater by chemically modified plant wastes as adsorbents: a review, *Biores. Technol.* 99 (2008) 3935–3948.
- [9] Y. Gao, Y. Wang, H. Zhang, Removal of Rhodamine B with Fe-supported bentonite as heterogeneous photo-Fenton catalyst under visible irradiation, *Appl. Catal. B: Env.* 78 (2015) 29–36.
- [10] V. Belessia, G. Romanosa, N. Boukosa, D. Lambropouloud, C. Trapalisa, Removal of Reactive Red 195 from aqueous solutions by adsorption on the surface of TiO₂ nanoparticles, *J. Hazard. Mater.* 170 (2009) 836–844.
- [11] A. Kurniawan, H. Sutiono, N. Indraswati, S. Ismadji, Removal of basic dyes in binary system by adsorption using rarasaponin–bentonite: Revisited of extended Langmuir model, *Chem. Eng. J.* 189–190 (2012) 264–274.
- [12] N. Belhouchat, H. Zaghouane-Boudiaf, C. Viseras, Removal of anionic and cationic dyes from aqueous solution with activated organo-bentonite/sodium alginate encapsulated beads, *Appl. Clay Sci.* 135 (2017) 9–15.

- [13] J. Chanathaworn, C. Bunyakan, W. Wiyaratn, J. Chungsiriporn, Photocatalytic decolorization of basic dye by TiO₂ nanoparticle in photoreactor, *Songklanakarin J. Sci. Technol.* 34 (2012) 203–210.
- [14] K. Nakataa, A. Fujishimaa, Design and applications, *J. Photochem. Photobiol. A: Chem.* 13 (2012) 169–189.
- [15] D.I. Petkowicz, R. Brambilla, C.U. Radtke, C.D.S. Silva, Z.N.d.R.B.C. Pergher, J.H.Z. Santos, Photodegradation of methylene blue by in situ generated titania supported on a NaA zeolite, *Appl. Catal. A* 357 (2009) 125–134.
- [16] B. Damardji, H. Khalaf, L. Duclaux, B. David, Preparation of TiO₂-pillared montmorillonite as photocatalyst Part I. Microwave calcination, characterization, and adsorption of a textile azo dye, *Appl. Clay Sci.* 44 (2008) 201–205.
- [17] A.B. Dukic, K.R. Kumric, N.S. Vukelic, Z.S. Stojanovic, M.D. Stojmenovic, S.S. Milosevic, L.L. Matovic, Influence of ageing of milled clay and its composite with TiO₂ on the heavy metal adsorption characteristics, *Ceramic Int.* 41 (2015) 5129–5137.
- [18] S. Ismadji, D.S. Tong, F.E. Soetaredjo, A. Ayucitra, W.H. Yu, C.H. Zhou, Bentonite hydrochar composite for removal of ammonium from Koi fish tank, *Appl. Clay Sci.* 119 (2016) 146–154.
- [19] K. Bahranowski, A. Gawel, A. Klimek, A. Michalik-Zym, B.D. Napruszewska, M. Nattich-Rak, M. Rogowska, E.M. Serwicka, Influence of purification method of Na-montmorillonite on textural properties of clay mineral composites with TiO₂ nanoparticles, *Appl. Clay Sci.* 140 (2017) 75–80.
- [20] J. Henych, M. Kormunda, M. Stastny, P. Janos, P. Vomacka, J. Matousek, V. Stengl, Water-based synthesis of TiO₂/CeO₂ composites supported on plasma-treated montmorillonite for parathion methyl degradation, *Appl. Clay Sci.* 144 (2017) 26–35.
- [21] E. Rossetto, D.I. Petkowicz, J.H.Z.d. Santos, S.B.C. Pergher, F.G. Penha, Bentonites impregnated with TiO₂ for photodegradation of methylene blue, *Appl. Clay Sci.* 48 (2010) 602–606.
- [22] F.P. Yesi, Y.H. Sisnandy, F.E. Ju, S. Soetaredjo, Ismadji, Adsorption of Acid Blue 129 from Aqueous Solutions onto Raw and Surfactant-modified Bentonite: Application of Temperature-dependent Forms of Adsorption Isotherms, *Ads. Sci. Technol.* 28 (2010) 847–868.
- [23] A. Kurniawan, A.N. Kosasih, J. Febrianto, Y.H. Ju, J. Sunarso, N. Indraswati, S. Ismadji, Utilization of rarasaponin natural surfactant for organo-bentonite

preparation: Application for methylene blue removal from aqueous effluent,
Chem. Eng. J. 172 (2011) 158–166.